Preliminary Results about the Catastrophic Earthquake of 7 September 1999 in Athens, Greece

G. A. Papadopoulos
G. Drakatos
D. Papanastassiou
I. Kalogeras
G. Stavrakakis
Institute of Geodynamics, National Observatory of Athens

INTRODUCTION

The catastrophic earthquake that hit the metropolitan area of Athens, Greece on 7 September, 1999 at 11:56:50.5 GMT has already been considered as the most important earthquake event in the modern history of Greece. In fact, it is the first moderate-to-strong shock (M_s = 5.9) ever reported to have occurred at such a small epicentral distance (D ≈18 km) from the historical center of the city and the first shock in the long history of Athens to cause casualties within its urban area. About 100 buildings collapsed, causing 143 casualties, while another 800 were injured. Search and rescue operations were conducted in more than twenty-five different locations. Preliminary estimations indicate that the number of buildings classified as "red", " yellow", and "green" after official inspection were 13,000, 62,000, and 110,000, respectively. "Red" indicates buildings either damaged beyond repair or heavily damaged but repairable; "yellow" indicates repairable, seriously damaged buildings; and "green" means not seriously damaged buildings. During the first days after the shock about 100,000 people were rendered homeless. More than 50 municipalities were affected, while the tangible loss caused is roughly estimated equal to about $3b U.S. From the point of view of economic loss it is the worst natural disaster reported in the modern history of Greece.

First reports about the earthquake were published by Papadopoulos *et al.* (1999) and Pavlides *et al.* (1999, 2000), while Tselentis and Zahradnik (2000) prepared a preliminary report on the aftershock monitoring. Here we present more detailed though still preliminary results. In the remainder of this report the 7 September 1999 shock is referred to as "the Athens earthquake" for reasons of brevity.

GEOLOGIC SETTING

The basement rocks in the active region are Paleozoic shales and sandstones in altered phylites and quartz conglomerates, Triassic–Jurassic crystalline limestones, dolomites, and a few outcrops of Cretaceous limestones and possibly Paleocene flysch of the Pelagonian geotectonic zone (IGME, 1980). In some places, as in the small depression of Fili (see below), Neogene formations overlie unconformably the basement formation and consist of alternating beds of marls, lacustrine limestone marls, and sandstones. Quaternary deposits are unconsolidated sandy-clayey soils, talus cones, and scree. Several pre-existing inherited structures, zones of weakness like Cretaceous and post-Cretaceous thrusts of Paleozoic formations to Triassic–Jurassic crystalline limestone and post-Alpide normal faults, characterize the tectonics of the area.

Normal faults with typical morphological expression cut mainly the pre-Neogene formations, affecting also Neogene deposits. The Thriassion Pedion (or Aspropyrgos) Fault, trending WNW–ESE and dipping southwest (Figure 1), is clearly visible in aerial photographs and LANDSAT images, although it is covered by typical talus cones and scree limiting to the north the Thriassion depression. The Fili normal fault, of WNW–ESE trend and southwest dip (Figure 1), is a secondary, almost parallel structure, lying 4–5 km to the north.

Pavlides *et al.* (1999, 2000) performed field observations on the Fili Fault after the Athens earthquake and were able to identify steep scarps, corresponding to neotectonic and possibly to active fault slips, as well as polished fault surfaces cutting mainly through basement crystalline limestone and occasionally through cemented limestone breccia. They made slickenside measurements on polished surfaces, not

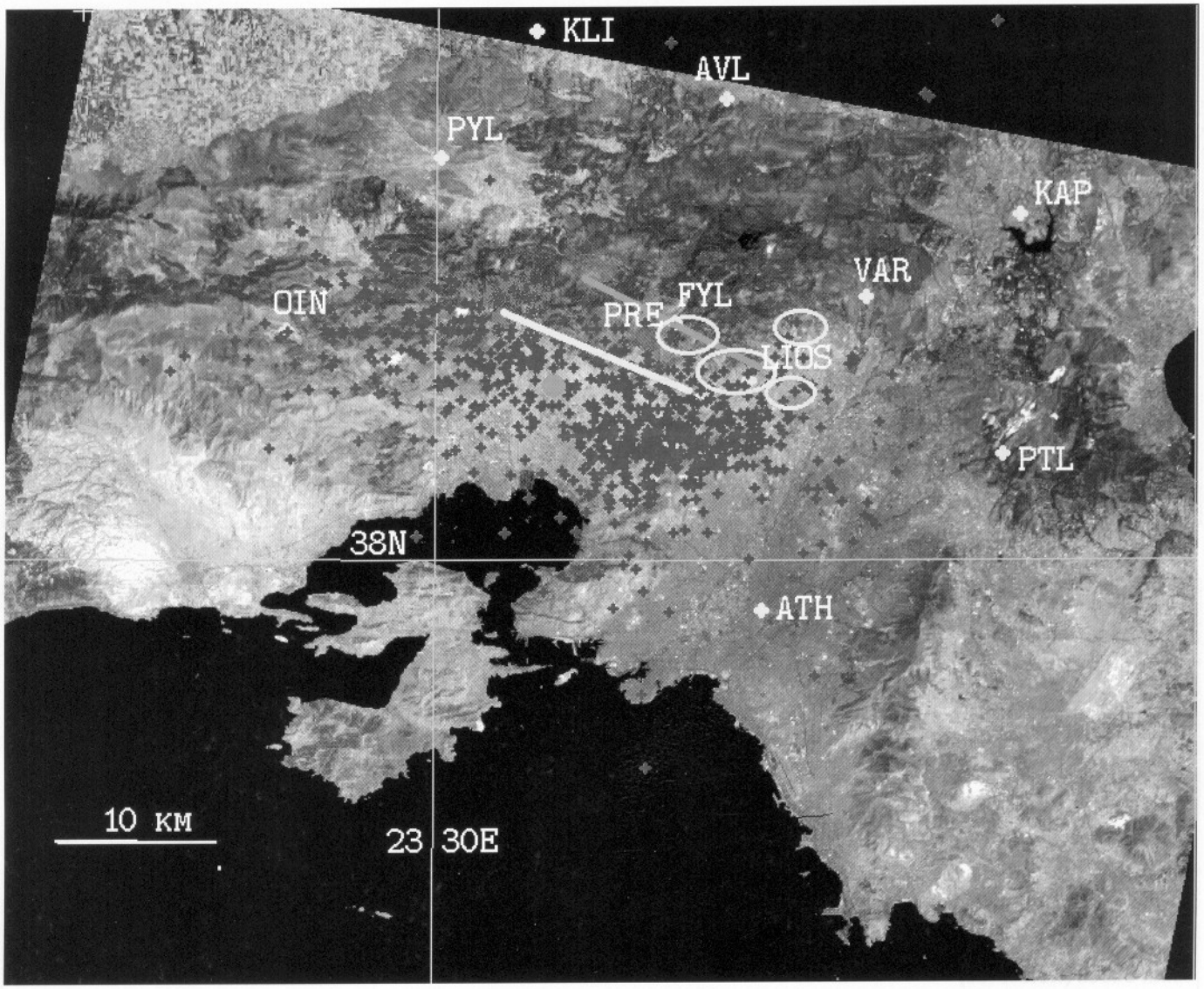

▲ **Figure 1**. Aftershock distribution according to determinations based on the NOAGI array recordings for the period 8 September to 29 October 1999. The Fili and the Thriassion Pedion (or Aspropyrgos) Faults are shown in a simplified way as blue and yellow lines, respectively. ATH and PTL are permanent seismograph stations of NOAGI, while the rest of the stations illustrated were installed after the main shock for the monitoring of the aftershock activity. The solid blue circle represents the relocated by NOAGI mainshock epicenter, while PRE shows the position of the preliminary NOAGI mainshock epicenter.

only on the master neotectonic fault but also on blocks separated by the Athens earthquake from the fault surface. Very young, normal dip-slip reactivation with the features strike N 110°–130°, dip SW 70°–80°, and pitches of striation or rake ranging from –76° to –88° were identified. A tensional stress field with the $\sigma 3$ axis trending NNE prevails in the area, which is consistent with the regional stress field derived from focal mechanisms and quantitative neotectonic fault analysis (Mercier *et al.*, 1989; Caputo and Pavlides, 1993).

Although no typical surface-fault traces appeared with the Athens earthquake, possible coseismic displacements ranging between 1 cm and 6 cm were observed by Pavlides *et al.* (1999, 2000) in at least three different locations along the Fili Fault, with the southwest fault segment moving downward with respect to the northeast segment. According to Coppersmith (1998), an earthquake of magnitude of the order of 6.0 has about 0.25 probability of producing surface ruptures. The Athens earthquake, therefore, was marginal in size for producing surface ruptures.

HISTORICAL SEISMICITY AND FORESHOCK ACTIVITY

Several strong earthquakes have been reported in the broad area surrounding Athens in historical times. From the macroseismic information available (Table 1) the earthquakes of 1705, 1805, and 1889 could be tentatively located at a distance of about 30 km from the center of Athens; however, there is no substantial evidence to support that even one of these events has been associated with the particular source

TABLE 1
Strong Historical Earthquakes and Small Instrumental Shocks Reported in the Vicinity of the 7 September 1999 Earthquake

YY	MM	DD	hh	mm	ss	Lat (N)	Long (E)	*Io*	*M*	Region	Ref
Historical earthquakes											
1705	09	03				38.2°	23.8°		≥ 6.0*	Athens	AJ97, PP97, PAP
1805	10	17	night			38.0°	23.7°	6?*		Athens	SM75, A94, PAP
1889	01	22	04	15		38.25°	23.75°	6		Athens	G53, G60
Instrumental shocks											
1965	04	03	05	19	21	37.0°	22.7°	4+	4 1/4	Athens	BNOA
1965	12	04	04	08	40	38.1°	23.8°	5	3.5	Attica–Ano Liosia	BNOA

The historical part of this table is an extract of the historical earthquake catalog for central Greece published by Papadopoulos *et al.* (2000). In this part of the catalog earthquake parameters have been adopted from the respective bibliographic references (Ref). Magnitudes marked by * were assessed by Papadopoulos *et al.* (2000). Key for the references: A94 = Ambraseys (1994), AJ97 = Ambraseys and Jackson (1997), BNOA = Bulletin of the Seismological Institute (1965), G53 = Galanopoulos (1953), G60 = Galanopoulos (1960), PAP = Papadopoulos *et al.* (1999), PP97 = Papazachos and Papazachou (1997), SM75 = Schmidt (1875).

TABLE 2
Earthquake Sequence of 7 September 1999

Date	Time (GMT)	Lat. (N)	Long. (E)	Depth (km)	M_L
Foreshocks					
1999 SEP 7	11 38 20.2	38.23°	23.47°	12	3.2
1999 SEP 7	11 40 10.6	38.06°	23.61°	10	2.5
1999 SEP 7	11 43 33.4	38.14°	23.42°	5	2.5
1999 SEP 7	11 54 42.6	37.98°	23.60°	11	3.2
Main Shock (Preliminary)					
1999 SEP 7	11 56 50.5	38.15°	23.62°	30	5.4
Main Shock (Relocated)					
1999 SEP 7	11 56 51.4	38.0°	23.58°	16.8	5.4
Largest Aftershock					
1999 SEP 7	20 44 55.0	38.19°	23.72°	21	4.4

that generated the 1999 Athens earthquake. In the instrumental era small magnitude shocks, like those of 3 April and 4 December 1965 (Table 1), were located very close to the epicenter of the 1999 Athens earthquake source as indicated by instrumental and macroseismic observations (Bulletin, 1965).

From the determinations of the permanent seismograph network of the National Observatory of Athens, Institute of Geodynamics (NOAGI), four events with local magnitude, M_L, of 3.2, 2.5, 2.5, and 3.2 were found to precede the main shock of 7 September 1999 within the last 18 minutes before the main shock occurrence (Table 2). These foreshocks were sizeable enough to be felt at places like Elefsina, Aspropyrgos, Moni Kliston, Fili, Ano Liossia, and Aharnes, in the area covered by the western aftershock cluster shown in Figure 1. However, reports from residents of places located further to the east, like Varibobi, Thrakomakedones, Dekelia, Kifisia, and Kapandriti, revealed that the foreshock activity was not felt at all by them. This macroseismic evidence indicates that the earthquake sequence possibly started in the western part of the activated area.

MAIN SHOCK AND ITS AFTERSHOCK SEQUENCE

According to the preliminary determination released by the NOAGI and the Geophysical Laboratory, University of Thessaloniki (GLUT), the main shock was a crustal (focal depth h = 30 km) moderate-to-strong event of M_L = 5.4 or M_s = 5.9 located at 38.15°N, 23.62°E (Table 2) at the northern segment of the Fili Fault, which dominates the southwest

foothills of Mount Parnitha (Figure 1). A preliminary USGS hypocentral determination indicated a shallower event (M_w = 5.9, M_0 = 7.8 × 10^{17} Nm, φ =38.13°N, λ = 23.54°E, h = 9 km). We relocated the main shock (Table 2) by including not only the NOAGI and GLUT data sets but also arrival times from stations belonging to the network of the Public Power Corporation (PPC). Moreover, arrival times of records from nine digital, 3-component, strong-motion instruments operated by NOAGI at different places throughout the city of Athens were incorporated. In these digital records the triggering times were considered to be the *P*-wave first arrivals. The relocated epicentral coordinates are 38.08°N, 23.58°E with a focal depth of 16.8 km; that is, the relocated epicenter has been shifted by about 15 km to the southwest and is at a shallower depth with respect to the preliminary one determined by NOAGI and GLUT.

The largest aftershock, of M_L = 4.4, occurred at 20:44:55.0 (GMT) on 7 September 1999 (Table 2). After the main shock one digital seismographic array and another analog seismograph array were deployed in the earthquake area. The analog array (Figure 1) consisted of eight portable, smoke-paper Sprengnether MEG-800 instruments equipped with S-13 short-period (1 Hz), vertical Teledyne seismometers. The preliminary results presented here about the aftershock sequence are based on the data obtained from the analog array as well as on recordings coming from the permanent NOAGI seismograph network, particularly from the stations ATH and PTL (Figure 1). Results obtained by the digital array will be presented elsewhere.

P-wave and *S*-wave phases recorded by the analog array as well as by ATH and PTL were used to locate about 1,030 aftershocks that occurred from 8 September to 29 October 1999. At least six phases have been used to determine focal parameters for each one of the aftershock events. A modification of the velocity model developed by Papadimitriou *et al.* (1999) for the area of Attika, the area within which the 1999 earthquake occurred, has been utilized. The modified model is Vp/h: 4.80/0.0, 5.40/4.0, 5.80/7.2, 6.30/10.4, 6.50/15.0, 7.00/30.0, where Vp is the *P*-wave velocity in km/sec and h is the depth in km. Duration magnitudes of $1.2 \leq M_D \leq 4.1$ were determined from signal duration calibration formulas based on recordings of the permanent NOAGI network.

The aftershock epicentral locations (Figure 1) imply that the major axis of the aftershock area strikes in a NNW–ESE direction, which is also the strike of both the Fili and Thriassion Pedion Faults and should be the direction of the seismogenic structure. As we will see later, this conclusion is consistent with the fault-plane solutions of the mainshock.

In Figure 1 it is clear that two main spatial aftershock clusters, the western and eastern ones, are recognizable with the epicenter density being clearly higher in the eastern area. Between the two clusters the aftershock activity is sparsely distributed, something that became clear from the first days of the activity. Cross-sections along the NNE–SSW and WNW–ESE directions (Figure 2) indicate that the rupture started with the main shock at the deeper part of the activated zone and then moved to shallower parts. The existence of an aseismic gap at the depth range of about 5 km to 7 km may delineate the presence of material of increased strength against failure, like a barrier. A section along a NNE–SSW direction, along the dip of the Fili geological fault, indicates that the zone of earthquake foci is of a length of about 15 km and a dip of about 80°, which is consistent with the dip measured by Pavlides *et al.* (1999) at the Fili Fault surface. Along a section trending WNW–ESE, along the major aftershock axis, the length of the zone of earthquake foci is about 25–30 km, while the density of earthquake foci at the eastern end is clearly higher with respect to that in the western part of the section.

The magnitude-frequency relation of Gutenberg and Richter (1944)

$$\log (N) = a - bM \qquad (1)$$

where N is the number of earthquakes of magnitude equal to or larger than M, and a and b are parameters of the distribution, has been examined on the basis of a complete sample of about 700 aftershocks of $M_D \geq 1.5$ or $M_s \geq 2.0$. The b value of (1) has been found by the least-squares approximation to be equal to 1.13 (Figure 3), which is a typical value for Greek aftershock sequences (Papazachos, 1974). The spatial distribution of the parameter b in the aftershock area (Figure 3) implies that values between 1.0 and 1.4 and even larger are associated with the central and eastern parts of the aftershock area, where the number of aftershocks and density of epicenters are higher with respect to those in the western part.

FAULT-PLANE SOLUTIONS

Preliminary fault-plane solutions determined teleseismically imply that the main shock rupture is associated with typical normal faulting, with the nodal planes having the following parameters: NP1 (strike/dip/slip): 292°/36°/–99° (USGS), 271°/47°/–106° (Harvard), 294°/47°/–83° (MEDNET); NP2 (strike/dip/slip): 123°/55°/–84° (USGS), 114°/45°/–73° (Harvard), 104°/43°/–97° (MEDNET). By using *P*-wave polarities from the permanent network of NOAGI as well from the networks of GLUT and PPC we were able to determine a fault-plane solution indicating normal faulting and nodal planes having directions 113°N and 290°N, dipping 56° to the northeast and 39° to the southwest, respectively (Table 3, Figure 4). This focal mechanism is in general agreement with the teleseismic ones mentioned above. Results of the geological field observations performed by Pavlides *et al.* (1999, 2000) as well as the spatial distribution of aftershocks shown in the cross-sections of Figure 2 leave no doubt that the fault plane dips to the SSW.

Focal mechanisms determined for thirty-eight aftershocks with magnitudes of $M_L \geq 2.6$ (Table 3, Figure 4) are generally consistent with the mechanism of the main shock. For some events, however, a significant strike-slip component is also evident.

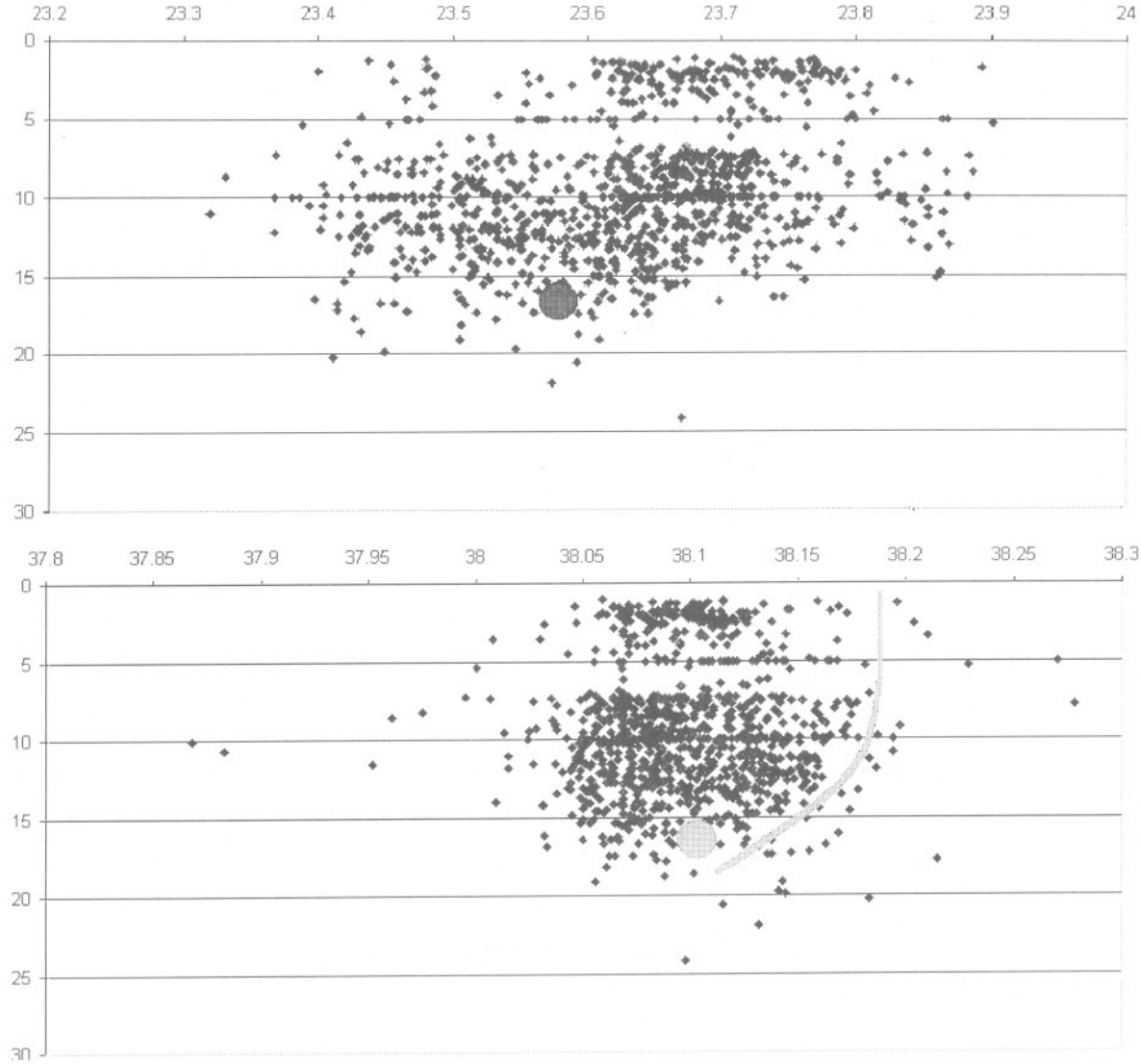

▲ **Figure 2.** Cross-sections of the aftershock foci. The large circle locates the main shock focus.

STRONG GROUND MOTION AND DAMAGE OBSERVED

In the meizoseismal area, located to the north and northwest of the city of Athens, the collapse of about 100 reinforced-concrete buildings, such as factory installations, flat blocks, and one-story or two-story houses, caused 143 casualties and about 800 injuries (Figures 5, 6, and 7). These collapses all occurred on the hanging-wall block of the Fili Fault. In this area a maximum intensity (modified Mercalli-Sieberg scale) of VIII, with local spots of IX, has been assigned to the towns of Fili, Ano Liossia, Aharnes, and Metamorphosis. Moreover, the main body of ground failures, like rockfalls and small-scale gravitational landslides, was observed along or very close to the Fili neotectonic fault (Pavlides *et al.*, 1999, 2000).

Unfortunately, strong-motion instruments were not operating in the meizoseismal area at the time of the Athens earthquake. A number of instruments, however, were operated by NOAGI at several places in the metropolitan area of Athens (Table 4, Figure 8), while additional strong-motion instruments were installed after the main shock. The installation places are different in geologic conditions as well as in the level of the structure of installation. The corrected peak ground acceleration due to the main shock varies between 0.5 g at the Monastiraki (MNSA) site in downtown to 0.075 g at the Dimokritos (DMK) site (Table 5). The instrument at the Monastiraki site was installed within the area of the work site of the new Athens subway, so extreme local conditions prevail. An archaeological shaft of quite large dimensions (30 m × 30 m) and a depth of approximately 30 m exists a little further away. Containers that were not anchored in any way and a high steel crane were also present. This complicated situation presumably affected the records of this specific site. In Dimokritos there is a typical rock, free-field site. Given the extreme local conditions in Monastiraki, the value of 0.31 g recorded at the Sepolia Gar (SPLB) station

TABLE 3
Fault-plane Solutions of the Athens Earthquake and Its Largest Aftershocks (see Figure 4) Determined on the Basis of the *P*-wave First-motion Onset

						Plane 1			Plane 2			*P* Axis		*T* Axis	
Date	Origin Time	Lat (N)	Long (E)	h(km)	M_L	Azm	Dip	Rake	Azm	Dip	Rake	Azm	Dip	Azm	Dip
1999 SEP 7	11:56:51.4	38.08°	23.58°	16.8	5.4	113°	39°	–90°	293°	51°	–90°	113°	6°	293°	84°
1999 SEP 7	17:19:21.8	38.11°	23.72°	16.2	4.2	114°	30°	–87°	290°	60°	–91°	105°	15°	291°	74°
1999 SEP 7	20:32:27.1	38.12°	23.63°	18.2	4.5	105°	45°	–30°	217°	69°	–130°	352°	41°	245°	75°
1999 SEP 8	03:21:32.5	38.09°	23.83°	14.1	4.0	106°	26°	–74°	268°	65°	–97°	73°	21°	274°	70°
1999 SEP 8	03:35:20.5	38.12°	23.89°	13.0	4.0	106°	30°	–74°	267°	61°	–99°	66°	17°	274°	74°
1999 SEP 8	12:55:1.0	38.14°	23.74°	19.9	4.4	330°	70°	–30°	71°	61°	–157°	198°	54°	292°	84°
1999 SEP 8	13:18:21.0	38.08°	23.79°	3.3	4.1	102°	38°	–78°	266°	52°	–99°	48°	10°	273°	82°
1999 SEP 8	16:50:37.8	38.19°	23.91°	1.4	4.0	113°	28°	–67°	267°	64°	–101°	64°	21°	276°	71°
1999 SEP 8	16:54:8.6	38.14°	23.79°	19.4	4.4	310°	50°	–20°	53°	74°	–138°	189°	50°	86°	74°
1999 SEP 8	21:58:52.5	38.15°	23.63°	13.0	3.1	300°	55°	–30°	48°	65°	–141°	178°	45°	81°	83°
1999 SEP 10	14:49:57.2	38.08°	23.81°	9.2	3.2	94°	38°	–90°	274°	52°	–90°	94°	7°	274°	83°
1999 SEP 12	06:17:42.3	38.16°	23.82°	13.8	3.5	60°	40°	–114°	270°	54°	–71°	142°	16°	256°	82°
1999 SEP 13	19:45:15.8	38.08°	23.75°	8.8	3.0	40°	56°	–110°	253°	38°	–63°	171°	18°	54°	81°
1999 SEP 16	08:12:10.5	38.10°	23.73°	7.9	3.7	66°	50°	–93°	250°	40°	–86°	223°	5°	68°	85°
1999 SEP 23	16:36:42.9	38.15°	23.62°	11.0	3.2	72°	50°	–95°	259°	40°	–84°	217°	6°	75°	85°
1999 SEP 25	20:46:34.2	38.12°	23.55°	5.3	3.4	100°	30°	–110°	302°	61°	–78°	147°	19°	294°	73°
1999 SEP 10	17:01:43.8	38.10°	23.68°	16.6	4.4	120°	55°	–50°	244°	51°	–132°	359°	31°	92°	87°
1999 SEP 11	10:23:8.7	38.03°	23.64°	10.3	4.4	90°	40°	–110°	295°	52°	–73°	167°	14°	284°	83°
1999 SEP 11	12:09:49.4	38.07°	23.62°	16.9	4.0	130°	55°	–40°	245°	58°	–137°	9°	38°	277°	88°
1999 SEP 12	11:19:8.3	38.05°	23.68°	8.9	4.3	110°	55°	–50°	234°	51°	–132°	349°	31°	82°	87°
1999 SEP 12	14:00:36.8	38.10°	23.76°	9.8	4.7	145°	45°	–70°	297°	48°	–108°	47°	14°	310°	88°
1999 SEP 12	17:23:24.7	38.04°	23.64°	14.0	4.8	85°	50°	–120°	306°	48°	–59°	197°	22°	105°	89°
1999 SEP 12	18:04:54.1	38.05°	23.78°	15.0	4.7	40°	45°	–100°	234°	45°	–80°	133°	7°	227°	89°
1999 SEP 12	21:34:45.8	38.07°	23.67°	8.9	4.4	140°	50°	–160°	36°	74°	–41°	260°	50°	3°	74°
1999 SEP 13	16:46:40.4	38.03°	23.69°	8.3	4.8	115°	50°	–40°	233°	60°	–132°	0°	36°	261°	83°
1999 SEP 14	03:18:30.5	38.05°	23.68°	17.6	4.9	150°	40°	–160°	44°	77°	–51°	262°	45°	16°	67°
1999 SEP 16	23:02:38.5	38.04°	23.67°	13.2	5.3	85°	45°	–120°	304°	52°	–63°	185°	21°	285°	86°
1999 SEP 17	23:40:18.8	38.15°	23.52°	13.4	4.8	20°	40°	–110°	225°	52°	–73°	97°	14°	214°	83°
1999 SEP 20	08:58:30.0	38.04°	23.70°	13.1	4.4	105°	55°	–80°	267°	36°	–103°	319°	12°	97°	80°
1999 SEP 20	18:49:46.1	38.11°	23.61°	9.8	4.5	60°	55°	–60°	194°	44°	–125°	297°	24°	39°	84°
1999 SEP 21	17:00:13.6	38.08°	23.68°	11.5	4.2	110°	55°	–60°	244°	44°	–125°	347°	24°	89°	84°
1999 SEP 22	03:19:21.5	38.10°	23.68°	11.7	4.5	105°	70°	–90°	285°	20°	–90°	284°	25°	104°	65°
1999 SEP 30	14:22:5.1	38.13°	23.63°	12.3	4.2	100°	45°	–90°	280°	45°	–90°	171°	0°	280°	90°
1999 OCT 3	17:03:34.3	38.12°	23.85°	15.0	5.8	145°	60°	–40°	257°	56°	–142°	19°	41°	112°	87°
1999 OCT 8	16:19:12.9	38.14°	23.76°	14.2	4.2	150°	70°	–50°	262°	43°	–150°	13°	41°	121°	74°
1999 OCT 15	10:48:23.7	38.10°	23.67°	25.6	5.6	115°	60°	–90°	295°	30°	–90°	294°	15°	114°	74°
1999 OCT 15	12:54:50.1	38.11°	23.68°	8.6	4.2	130°	45°	–60°	270°	52°	–116°	29°	21°	289°	86°
1999 OCT 21	21:57:40.8	38.12°	23.56°	14.1	4.7	110°	65°	–60°	236°	38°	–136°	332°	31°	88°	75°

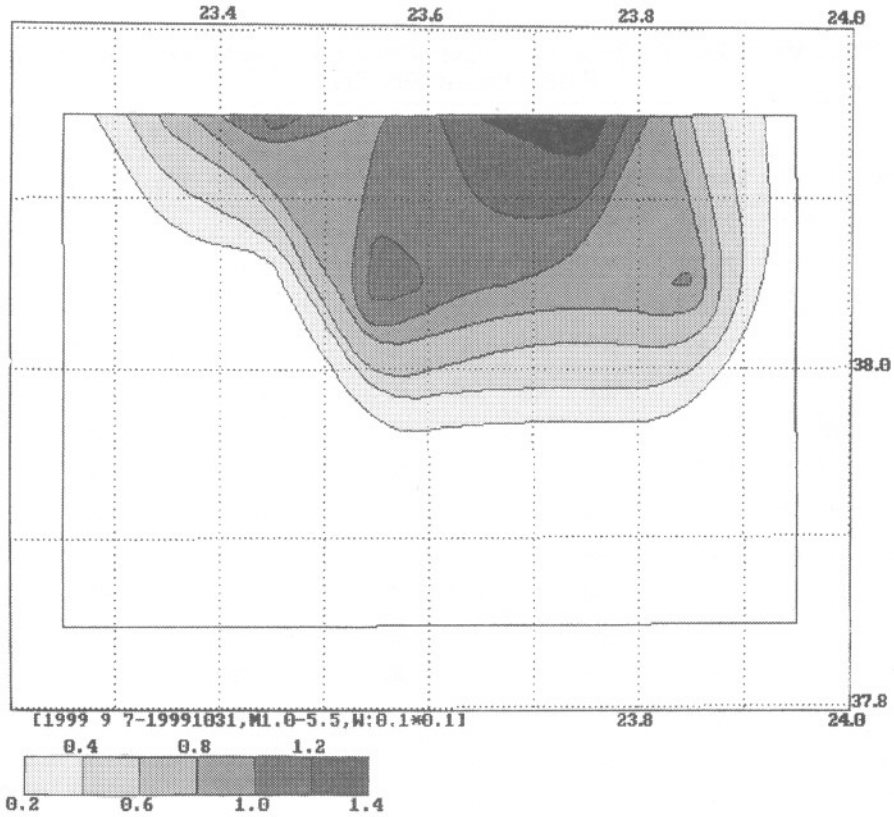

▲ **Figure 3**. Geographical distribution of the parameter b for the aftershock sequence. Solid black indicates $b \geq 1.4$. Large values are observed in the central and eastern parts of the aftershock areas.

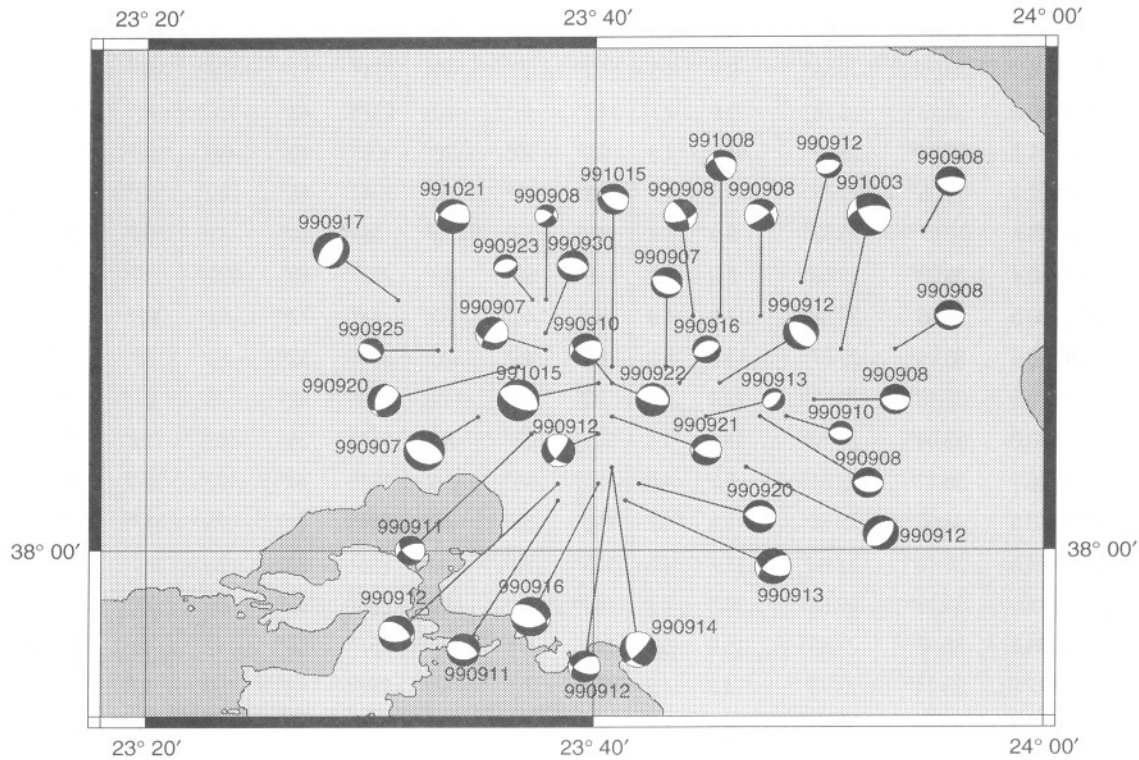

▲ **Figure 4.** Focal mechanisms determined for the main shock (M) of 7 September 1999 and its largest aftershocks on the basis of the P-wave first-motion onset (see Table 3).

▲ **Figure 5.** Rescue operation at the Fourlis factory installation in Kato Kifisia, the front part of which collapsed.

▲ **Figure 6.** Partial collapse of a three-story house in Aharnes.

▲ **Figure 7.** Partial collapse of a small two-story factory installation in Aharnes.

TABLE 4
Characteristics of Strong-motion Instruments That Recorded the 7 September 1999 Main Shock

Station	Location	Lat (N)	Long (E)	Site	Building	Geology	Orientation[a]
ATHA	NEO PSIHIKO	38.00°	23.77°	Private building	3-story RC	Tertiary deposits	N180°
ATHB	PAL. FALIRO	37.93°	23.70°	Planetarium	3-storey RC	Holocene deposits	N120°
DFNA	DAFNI	37.95°	23.74°	Subway station	–2 level (–14 m)	Alluvium/schist	N155°
DMK	AG. PARASKEVI	37.99°	23.82°	Dimokritos	Small RC house	Limestone	N135°
FIX	SYGROU-FIX	37.96°	23.73°	Subway station	–2 level (–15 m)	Alluvium/schist	N140°
MNSA	MONASTIRAKI	37.98°	23.73°	Subway station	Free field	Manmade deposits	N10°
PNT	PAPAGOS	38.00°	23.79°	Subway station	–2 level (–15 m)	Tertiary deposits	N135°
RFN	RAFINA	38.02°	23.00°	Private building	Small wooden house	Tertiary deposits/limestone	N250°
RNT	RENTIS	37.96°	23.68°	Town Hall	2-story RC	Alluvium/schist	N210°
SGMA	SYNTAGMA	37.98°	23.74°	Subway station	–1 level (–7 m)	Schist	N10°
SGMB	SYNTAGMA	37.98°	23.74°	Subway station	–3 level (–26 m)	Schist	N135°
SPLA	SEPOLIA	38.00°	23.71°	Subway station	–2 level (–13 m)	Alluvium/schist	N320°
SPLA	SEPOLIA	38.00°	23.71°	Subway garage	3-story steel building	Manmade deposits	N320°
THVC	THIVA	38.32°	23.32°	Town Hall	3-story RC	Pleistocenic deposits	N180°

a. The station orientation refers to the longitudinal component of the instrument.

can be considered as the most representative maximum processed acceleration measured. The local conditions as well as the azimuthal distribution of the radiation of the seismic energy seem to affect drastically the recorded strong ground motions, given that the epicentral distances of most of the stations are almost the same and equal to about 15 km.

DISCUSSION AND CONCLUSIONS

The Athens earthquake (M_s = 5.9) of 7 September 1999 was a very destructive, fatal event. Its meizoseismal area, characterized by macroseismic intensities of up to IX degree (MM), was located very close to the Fili neotectonic fault in the hanging-wall domain, where peak ground accelerations up to at least 0.31 g were recorded.

The spatial distribution of aftershocks along with the focal mechanism of the main shock leave no doubt that this earthquake was genetically associated with a WNW–ESE trending and SSW-dipping seismogenic structure, the topographic expression of which, possibly, is the neotectonic Fili Fault, striking 110°–130°N and dipping 60°–85°SW. Moreover, the position of the relocated main shock focus was at a depth of 16.8 km at a distance of about 15 km to the southwest from the surface trace of the Fili Fault, while the most important ground failures concentrate along the surface zone of the same fault.

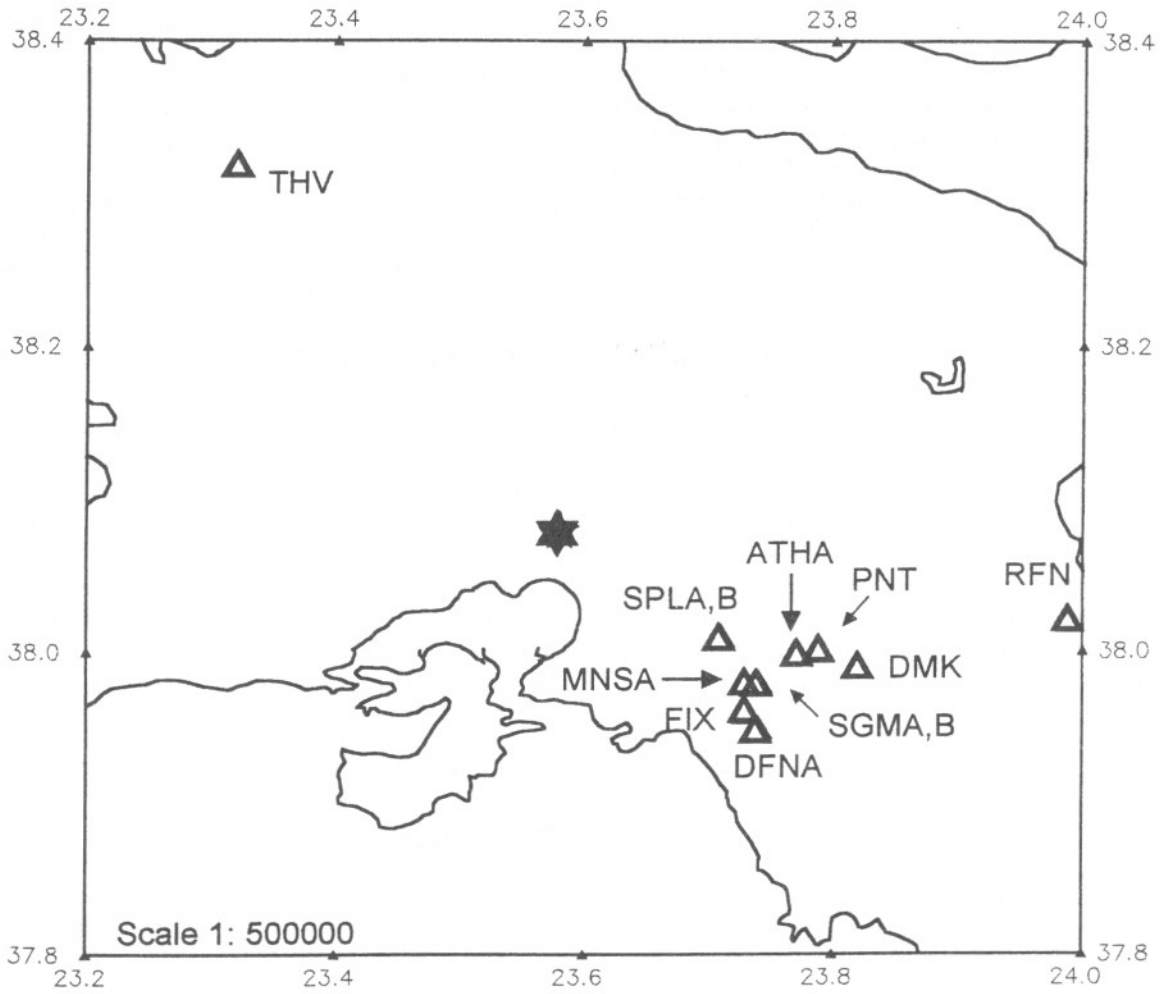

▲ **Figure 8.** Locations of the strong-motion instruments that recorded the 7 September 1999 main shock. The star illustrates the main shock epicenter.

TABLE 5
Strong Motion Peak Values of the 7 September 1999 Main Shock

Code	Type / S.N.	Location	Distance (km)	L-Accel cm/s/s	L-Veloc cm/s	L-Displ cm	V-Accel m/s/s	V-Veloc cm/s	V-Displ cm	T-Accel cm/s/s	T-Veloc cm/s	T-Displ cm
ATHA	A800/130	Neo Psihiko	22	81.99	5.35	1.33	112.1	3.37	0.68	98.69	7.48	1.25
DFNA	SMA1/1197	Dafni	23	43.66	4.35	1.04	40.06	2.71	0.47	78.61	7.52	2.14
DMK	A800/128	Ag. Paraskevi	26	45.05	2.41	0.79	36.84	3.00	0.68	46.46	2.47	0.46
FIX	A800/099	Sygrou-fix	22	84.19	7.88	1.71	44.75	3.51	0.75	121.9	10.93	1.95
MNSA	SMA1/4342	Monastiraki	20	224.90	14.84	3.79	158.95	3.31	0.47	501.94	14.64	2.17
PNT	A800/075	Papagos	23	86.46	7.55	1.60	54.22	3.77	0.96	77.55	5.10	0.76
RFN	SMA1/2711	Rafina	39	79.30	3.49	1.01	29.47	2.99	1.15	97.91	5.11	1.56
SGMA	A800/081	Syntagma	21	145.9	12.63	2.56	53.02	3.00	0.86	234.5	13.46	1.27
SGMB	A800/062	Syntagma	21	108.8	10.01	1.11	86.93	3.63	0.73	85.72	10.71	2.29
SPLA	A800/117	Sepolia	16	241.1	17.90	1.49	80.60	5.87	1.20	216.6	12.88	2.71
SPLB	A800/140	Sepolia	16	215.3	21.53	2.50	188.5	7.32	1.28	306.3	18.60	2.44
THVC	A800/106	Thiva	35	56.54	3.52	0.37	43.07	1.90	0.13	54.88	2.62	0.27

The foreshock locations imply that the earthquake sequence started in the western part of the activated zone. The mainshock rupture occurred in the deep (~17 km) central part of the aftershock zone and the aftershock activity continued at shallower levels mainly at the eastern part of the activated zone. This pattern implies a possible directivity of the mainshock rupture from southwest to northeast and upward, which may explain in part the heavy damage observed on the central and eastern sides of the activated zone. However, local ground conditions certainly contributed to the high ground accelerations and damage observed.

The b value of 1.13 found for the aftershock sequence and the magnitude difference of $M_0 - M_1 = 1.0$ between the main shock and its largest aftershock are typical for Greek shallow earthquakes. It is worth noting that the spatial distribution of the parameter b exhibits high values of $b = 1.0$ to 1.4 and even larger in the central and eastern parts of the aftershock area, where the number of aftershocks and the epicenter density were higher than those in the western part.

The Athens earthquake is very significant for three main reasons. The first is that never in the historical past is an earthquake of such a size known to have occurred so close to the city center of Athens. From this point of view the 7 September 1999 earthquake opens a new chapter in the seismic history of the city of Athens and raises new questions about the effectiveness of the seismic safety policy that hitherto has been based on the notion that the metropolitan area of Athens is not threatened by local earthquake sources.

The second reason that makes the 1999 Athens earthquake significant is that this event constitutes one more example of the earthquakes that are of only a rather moderate size but still cause destructive consequences because of their occurrences within or very close to urban areas. In Greece, another two similarly moderate yet destructive shocks occurred on 13 September 1986 at Kalamata (M_s = 6.2; 20 casualties) and on 15 June 1995 at Aeghio (M_s = 6.2; 26 casualties), both associated with normal faulting and with the main damage zone located on the hanging-wall block. In San Salvador the moderate (M ~5.4) shock of 10 October 1986 caused 1,500 casualties and 10,000 injuries. From the point of view of economic loss, the Athens earthquake was the worst natural disaster in the long history of Greece.

Last but not least, the Athens earthquake was rather unexpected in the sense that the particular seismogenic structure on which the earthquake apparently occurred was not considered to have a seismic potential beforehand. Pavlides *et al.* (1999, 2000) believe that this shock can be characterized as a "floating" or "random" event according to the terminology of De Polo and Slemmons (1990). In other words, the Athens earthquake originated from an unidentified seismogenic structure between other known faults of large or medium size. This is only one case among many other events of this type, like Tangshan (M_s = 7.8), China, 28 July 1978; Landers (M_s = 7.4), California, 28 June 1992; Kobe (M_s = 7.2), 17 January 1995; and Kozani-Grevena, Greece (M_s = 6.5), 13 May 1995 earthquakes.

From the Athens earthquake one may conclude that there is a general need to promote further research toward the identification of the earthquake potential associated with less studied seismogenic structures of even small or medium-size lying close to urban areas. This need is urgent for metropolitan areas, like that of Athens, where the total earthquake risk is extremely high because of the large population density, the relatively high vulnerability of structures, and the large economic value exposed to the earthquake activity (Papadopoulos and Arvanitides, 1996).

ACKNOWLEDGMENTS

This paper has been written within the frame of the research project ASPELEA (Assessment of Seismic Potential in European Large Earthquake Areas), supported by the Commission of European Communities – DG XII, INCO – COPERNICUS Program, contr. n. IC – 15CT – 97 – 0200, and partly by the General Secretary of Research and Technology, Greece. We thank Dr. A. Ganas for plotting the data of Figure 1 on a LANDSAT satellite image, Dr. N. Voulgaris for helping in the construction of Figure 4, and A. Plessa for her help in the analysis of the aftershock records. Thanks are due to Dr. J. Ebel, who made comments and editorial corrections that improved the original manuscript.

REFERENCES

Ambraseys, N. N. (1994). Material for the investigation of the seismicity of central Greece. in *Historical Investigation of the Seismicity of European Earthquakes*, Albini, P. and A. Moroni (eds.) **2**, 1–10.

Ambraseys, N. N. and J. A. Jackson (1997). Seismicity and strain in the Gulf of Corinth (Greece) since 1694, *J. Earthq. Eng.* **1**, 433–474.

Bulletin, Seismological Institute, National Observatory of Athens, April and December, Athens, 1965.

Caputo, R. and S. Pavlides (1993). Late Cenozoic geodynamic evolution of Thessaly and surroundings (central-northern Greece), *Tectonophysics* **223**, 339–362.

Coppersmith, K. (1998). Seismic source characterization: Closing the gap between earthquake sciences and seismic hazard analysis, *Int. Workshop on Active Faults, Camerino, June 4–6, 1998*, 39–40.

De Polo, M. C. and B. D. Slemmons (1990). Estimation of earthquake size for seismic hazards, *Geol. Soc. Amer. Rev. Eng. Geol.* **VIII**, 1–28.

Galanopoulos, A. G. (1953). Katalog der Erdbeben in Griechland für die Zeit von 1879 bis 1892, *Ann. Geol. Pays Hellen.* **5**, 144–229 (in German with Engl. abstr.).

Galanopoulos, A. G. (1960). *Greece: A Catalogue of Shocks with Io ≥ VI or M ≥ 5 for the Years 1801–1958*, Seism. Lab. Univ. Athens.

Gutenberg , B. and C. Richter (1944). Frequency of earthquakes in California, *Bull. Seism. Soc. Am.* **34**, 185–188.

IGME (1980). *Geological Map of Greece: Athinai–Elefsis* (1:50,000), Inst. of Geology and Mining Exploration, Athens.

Mercier, J.-L., D. Sorel, P. Vergely, and K. Simeakis (1989). Extensional tectonics regimes in the Aegean Basins during the Cenozoic, *Basin. Res.* **2**, 49–71.

Papadimitriou, P., G. Kaviris, and K. Makropoulos (1999). Evidence of shear-wave splitting in the eastern Corinthian Gulf (Greece), *Phys. Earth Planet. Inter.* **114**, 3–13.

Papadopoulos, G. A. and A. Arvanitides (1996). Earthquake risk assessment in Greece, in *Earthquake Hazard and Risk,* Schenk, V. (ed.), Kluwer Academic Publ., 221–229.

Papadopoulos, G. A., I. Baskoutas, G. Chouliaras, G. Drakatos, I. Kalogeras, V. Karastathis, M. Kourouzidis, I. Latoussakis, D. Makaris, N. Melis, G. Panopoulou, D. Papanastassiou, I. Pappis, S. Tassos, A. Plessa, and G. Stavrakakis (1999). Seismological aspects of the Athens earthquake of 7th September, 1999: Preliminary results, *1st Conf. Advances in Natural Hazards Mitigation: Experiences from Europe and Japan, Programme – Abstracts–Reports*, Athens, 3–4 November, 1999, 73–79.

Papadopoulos, G. A., A. Vassilopoulou, and A. Plessa (2000). *A Catalogue of Historical Earthquakes for Central Greece: 480 B.C.–1910 A.D.*, Institute of Geodynamics, National Observatory of Athens, Publ. No. 11.

Papazachos, B. C. (1974). On certain aftershock and foreshock parameters in the area of Greece, *Annali Geofisica* **27**, 497–515.

Papazachos, B. C. and K. Papazachou (1997). *The Earthquakes of Greece*, Zitti Publ., Thessaloniki, 304 pp.

Pavlides, S., G. A. Papadopoulos, and A. Ganas (1999). The 7th September, 1999 unexpected earthquake of Athens: Preliminary results on the seismotectonic environment, *1st Conf. Advances in Natural Hazards Mitigation: Experiences from Europe and Japan, Programme—Abstracts–Reports*, Athens, 3–4 November, 1999, 80–85.

Pavlides, S., G. A. Papadopoulos, and A. Ganas (2000). Seismic hazard in urban areas: The 7th September 1999 Athens earthquake case study, in *Proc. of the Hokudan Int. Symp. and School on Active Faulting: Active Fault Research for the New Millennium, Jan. 17th–26th, 2000,* Okumura, K., K. Takada, and H. Goto (eds.), 367–370.

Schmidt, J. (1875). *Studien über Erdbeben*, Leipzig, 324 pp.

Toksöz, M. N., Reilinger, R. E., Doll, C. G., Barka, A. A., and Yalcin, N. (1999). Izmit (Turkey) earthquake of 17 August 1999: First report, *Seism. Res. Lett.* **70**, 669–679.

Tselentis, G.-A. and J. Zahradnik (2000). Aftershock monitoring of the Athens earthquake of 7 September 1999, *Seism. Res. Lett.* **71**, 330–337.

Institute of Geodynamics
National Observatory of Athens
P.O. Box 20048
GR-118 10 Athens
Greece
e-mail: **g.papad@egelados.gein.noa.gr**